ELSEVIER

Thermochimica Acta 401 (2003) 95–109

thermochimica acta

www.elsevier.com/locate/tca

Structural evolution upon heating of sol–gel prepared birnessites

O. Prieto, M. del Arco, V. Rives*

Departamento de Química Inorgánica, Universidad de Salamanca, Salamanca 37008, Spain

Received 22 July 2002; accepted 13 October 2002

Abstract

Birnessites containing K^+ and Na^+ in the interlayer have been prepared by a sol–gel method using glucose and polyvinyl alcohol as reducing agents. The samples have been characterised by elemental chemical analysis, powder X-ray diffraction, thermal analysis (differential and thermogravimetric), FT-IR spectroscopy and specific surface area and texture assessment by nitrogen adsorption at −196 °C. The solids obtained are more crystalline than those prepared by oxidation with H_2O_2 in a basic medium. The samples are thermally stable and evolution upon calcination at high temperature depends on the precise nature of the interlayer cation. So, calcination at 600 °C of a K-birnessite leads to formation of cryptomelane (2 × 2 tunnel structure), while the Na analogue leads to formation of mixed Mn–Na oxides with different tunnel structures. Ion exchange of interlayer cations takes place topotactically at room temperature; Li^+ enters easily in the interlayer, while the entrance of Mg^{2+} is more difficult, probably because of its high stability in the hydrated form; increasing of the temperature and contacting time during ion exchange does not improve very largely the process.

Keywords: Birnessite; Ion exchange; Thermal analysis

1. Introduction

Birnessite is a common name for layered manganese oxides, formed by bidimensional layers of edge-sharing MnO_6 octahedra, with metal cations (usually alkaline or alkaline-earth cations) in the interlayer, together with water molecules; these cations balance the negative electric charge of the layers because of the partial reduction of Mn ions below the +4 state [1–11]; a sketch of this structure is depicted in Fig. 1. The structural formula can be written as $A_xMnO_{2\pm y}{\cdot}z(H_2O)$, where A stands for the interlayer cation. The oxidation state of manganese ranges between 3.6 and 3.8, indicating that it mostly corresponds to Mn(IV), and Mn(III) in a lower extent. The common interlayer spacing for samples containing interlayer alkaline or alkaline-earth cations is close to 7 Å, but upon hydration it can increase up to 10 Å, the solid then being known as busserite. A complete dehydrated sample, with an interlayer spacing of 5.5 Å, is also known [10]. These solids undergo ion exchange of the interlayer cations, such a process usually leading to changes in the interlayer spacing.

Birnessites have been identified in nature in deep sea manganese nodules [12–14], and different synthetic routes have been described to prepare birnessites [3–7,12–21].

Calcination of birnessites leads to formation of solids with many different structures, but mainly cubic spinels and tunnel structures, which present many potential applications; Mn–Li spinels are used as cathodes in rechargeable batteries [3,13,22–26]. Some other are interesting because of their magnetic [27]

* Corresponding author. Fax: +34-923-294574.
E-mail address: vrives@usal.es (V. Rives).

0040-6031/03/$ – see front matter © 2002 Elsevier Science B.V. All rights reserved.
PII: S0040-6031(02)00503-8

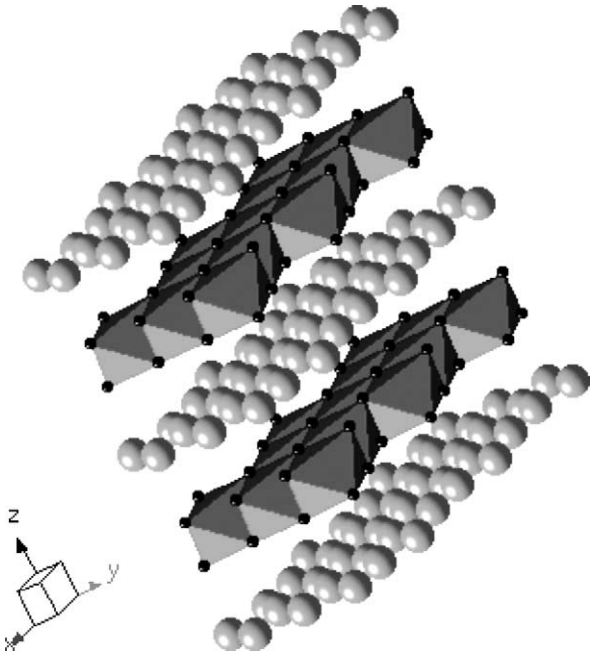

Fig. 1. Structure of birnessite.

or electrochemical properties, and have been used as molecular and ionic sieves [1,28], catalysts [29], etc.

The properties of these layered materials depend in some way on the synthetic route followed to prepare them and on the specific nature of the interlayer cation. Such differences can originate from different particle size or to the type and concentration of lattice defects; consequently, small changes in the synthetics parameters can lead to formation of solids with different catalytic, electrochemical or ion exchange properties.

In the present paper, we report on the preparation and characterisation of birnessites containing K^+ or Na^+ as the interlayer cation, as well as their ionic exchange properties (Li^+, Cu^{2+}, and Mg^{2+}). Formation of solids with tunnel structures upon calcination of these solids is also reported.

2. Experimental

2.1. Samples preparation

All chemicals were from Fluka (Switzerland). Gases were from L'Air Liquide (Spain) with nominal purities of 99.9990%, and were used without further purification.

2.1.1. Sol–gel method

The method followed was essentially similar to that described by Ching et al. [9,10]. A portion (100 ml) of an aqueous solution (0.27 M) of $KMnO_4$ or $NaMnO_4{\cdot}H_2O$ is added to a solution containing 5.04 g glucose(+) in 70 ml water (0.40 M); in these cases, the glucose/interlayer cation molar ratio was ca. 1:1. A sodium-containing sample was prepared with a glucose/cation molar ratio close to 1.5 by adding 50 ml of an aqueous $NaMnO_4{\cdot}H_2O$ solution (0.38 M) to 20 ml of a 1.4 M solution of glucose. In any case, the resulting solution was vigorously stirred using a magnetic stirrer for a short period of time (20 s for the K samples, and 40–60 s for the Na samples) and then left standing at room temperature. A brown gel was formed, the reaction being exothermic, while water is liberated and the gel slightly shrinks; water was removed by decantation during ca. 1 h and then the gel was dried in an open oven at 110 °C overnight; this led to formation of a dark, almost black, brown xerogel, which was calcined in air at 400 °C for 2 h. The almost completely black solid thus obtained was washed with water several times, by suspension in distilled water and centrifugation, and then was dried at 100 °C overnight.

Another K-containing birnessite was prepared using polyvinyl alcohol as a reducing agent, instead of glucose. Five grams of polyvinyl alcohol were dissolved in 40 ml of distilled water, and then 50 ml of a 0.38 M solution of $KMnO_4$ were added. The suspension was vigorously stirred for 90 s until the exothermic reaction started, and then was left standing to cool; drying, washing and calcination were performed as above described for the samples prepared using glucose.

2.1.2. Ion exchange

This method was used to insert Li^+, Cu^{2+} and Mg^{2+} in the interlayer space of the samples prepared following the sol–gel method. For this, 0.5 g of the starting birnessite (in the Na or K form) were dispersed in 100 ml of a 1 M solution of Cu or Mg nitrate or LiCl in distilled water. The suspension was magnetically stirred at room temperature for 24 h, washed by centrifugation with distilled water and the solids were filtered and dried at 110 °C overnight.

Several samples were prepared also by ion exchange of the K-birnessite, but at 80 °C, reducing the exchange time to 3 or 8 h, and increasing the concentration of the salt to 1.5 M.

2.1.3. Calcined systems

The samples prepared were calcined in air at 600 or 1000 °C for 2 h; these temperatures were selected after analysing the thermal properties of the solids prepared.

2.1.4. Naming of the samples

A letter is used to indicate the reducing agent (G for glucose, V for polyvinyl alcohol), followed by the chemical symbol of the interlayer cation (K, Na) and the molar glucose/cation ratio used during synthesis. An additional "I" and the symbol of the entering cation denotes the samples prepared by ion exchange and, finally, the calcination temperature is added for the calcined systems.

2.2. Characterisation of the samples

Mn, Na, K, Cu, Mg, Li were analysed in Servicio General de Análisis Químico Aplicado (Universidad de Salamanca, Spain) by atomic absorption in a Mark 2 ELL-240 instrument, after dissolving the samples in hydrochloric acid.

The powder X-ray diffraction (PXRD) diagrams were collected in a model D500 Siemens diffractometer, with Cu Kα radiation ($\lambda = 1.54050$ Å) and graphite monochromator; the filament current was fixed to 30 mA and the potential difference to 40 kV; the diagrams were recorded at a scanning speed of 2° (2θ)/min, with a collection time of 1.5 s. The data stored at the JCPDS [30] data base were used to identify the crystalline species existing in the samples.

Differential Thermal Analyses were carried out in a DTA7 instrument from Perkin-Elmer, and thermogravimetric analyses (TG) were recorded on a TG7 thermobalance from Perkin-Elmer; both are connected to a Dell computer, controlling both instruments through Pyris software, also from Perkin-Elmer; the analyses were carried out at a heating rate of 10 °C/min, the sample being surrounded by a dynamic (20 ml/min) atmosphere of oxygen.

The FT-IR spectra of the samples were recorded using the KBr pellet technique in a Perkin-Elmer FT1730 spectrometer in the 4000–400 cm^{-1} range, averaging 100 scans with a nominal resolution of 2 cm^{-1}, to improve the signal-to-noise ratio.

Specific surface areas of the samples were determined, as well as their surface texture properties, from the N_2 adsorption-desorption isotherms, recorded at −196 °C in a Gemini instrument from Micromeritics; the samples had been degassed previously at 150 °C for 2 h in a FlowPrep 060 apparatus, also from Micromeritics. The specific surface area was determined following the BET method [31], and other literature methods were also applied to determine the cumulative surface area, pore size distribution curves and the *t*-plots; such analysis was carried out using published software [32].

3. Results and discussion

3.1. Elemental chemical analysis

The structural formulae of the solids prepared are included in Table 1. In all cases, they have been written assuming an initially stoichiometric composition MnO_2 and the absence of anion vacancies or the presence of deffect OH groups isomorphically substituting oxide anions, and have been calculated from the elemental chemical analysis data for the metals present. The amount of water has been calculated from the two first weight losses recorded in the TG curves (see below). The Na and K contents, for the samples prior to ion exchange, are similar to those reported previously by other authors [9]. The sodium content, however, is ca. 50% larger than that of potassium, probably because of a different redox mechanism during synthesis, related to their different ionic radii. The content of interlayer water is also similar to that reported previously for birnessites prepared following this same method, although the values are larger than those found for samples prepared following the oxidation method in basic medium [3–7,33].

The average oxidation state of manganese can be calculated from these formula, assuming no lattice defects (i.e. O^{2-}/OH^{-} substitution). The values calculated are 3.81 and 3.67, respectively, for the K- and Na-containing birnessites. These values are within the values reported in the literature for this sort of material.

Table 1
Structural formulae and specific surface area of the samples prepared

Sample	Mn[a]	K/Na[a]	A[a]	Formula	S_{BET} (m^2/g)
GK1	55.4	7.5		$K_{0.190}$ MnO_2·0.35 H_2O	16
GK1IMg	54.9	5.2	0.72	$K_{0.132}$ $Mg_{0.030}$ MnO_2·0.51 H_2O	19
GK1ICu	53.9	1.4	4.84	$K_{0.036}$ $Cu_{0.078}$ MnO_2·0.71 H_2O	27
GK1ILi	57.2	0.47	1.3	$K_{0.012}Li_{0.180}$ MnO_2·0.77 H_2O	44
GNa1	50.9	7.04		$Na_{0.33}$ MnO_2·0.91 H_2O	29
GNa1IMg	52.2	3.5	2.0	$Na_{0.160}$ $Mg_{0.086}$ MnO_2·0.97 H_2O	33
GNa1ICu	49.5	0.24	9.2	$Na_{0.012}$ $Cu_{0.160}$ MnO_2·1.27 H_2O	33
GNa1ILi	53.1	0.1	2.2	$Na_{0.005}Li_{0.325}$ MnO_2·0.90 H_2O	60
GNa1.5	51.8	7.2		$Na_{0.33}$ MnO_2·0.70 H_2O	32
GNa1.5IMg	49.8	2.9	2.1	$Na_{0.138}Mg_{0.096}MnO_2$·0.99 H_2O	37
GNa1.5ICu	47.4	0.14	8.8	$Na_{0.007}Cu_{0.161}$ MnO_2·1.03 H_2O	33
GNa1.5ILi	52.3	0.20	2.1	$Na_{0.009}$ $Li_{0.321}$ MnO_2·0.87 H_2O	55

[a] Weight(%); A: Mg, Cu or Li.

3.2. Powder X-ray diffraction

The PXRD diagrams of representative samples are shown in Fig. 2. All they show two intense diffraction maxima close to 7.0 and 3.5 Å, characteristic of layered birnessite [9,13,14,34,35]. In addition, some diffraction lines in the 2θ (Cu Kα) range 32–56° are also observed; the maximum close to $2\theta = 60°$ is also

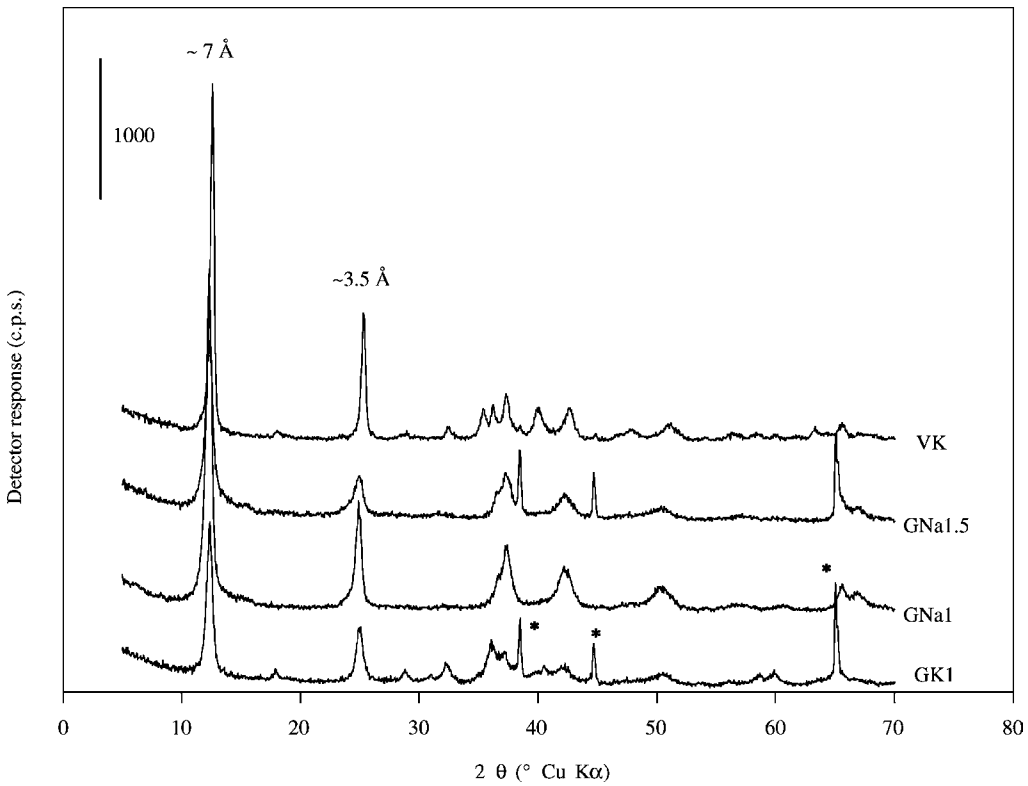

Fig. 2. XRD patterns of the original samples ((*) peaks of Al sample holder). The patterns have been displaced vertically for clarity.

characteristic of birnessite. In the case of both samples containing K^+ ions in the interlayer, some weak peaks corresponding to manganese oxides impurities are also recorded. The samples containing potassium seem to be more sensitive than the sodium ones to changes in the relative concentrations of the reagents during synthesis following this sol–gel method [10]; formation of gels, which undergo transformation to the layered structures upon heating, is favoured for relatively concentrated solutions, while incipient formation of manganese oxides with tunnel structures or even Mn_2O_3 (with a sesquioxide C structure) are obtained for low glucose/$KMnO_4$ ratios [9].

The PXRD diagrams (not shown) of the Na-containing samples indicate the presence of a mixture of two phases, both with layered structures, with basal spacings of 7 and 5.5 Å, which are originated by normal and dehydrated birnessite, respectively. Coexistence of these two phases has been previously reported in several studies [9,10,18], and, in our case, if the sample was suspended in water and shaken during 1 day, total re-hydration is achieved and the peak at 5.5 Å is not further recorded in the PXRD diagram (Fig. 2).

On comparison of all four PXRD diagrams, it can be observed that the diagrams for the Na-containing samples are "cleaner", i.e. they contain less diffraction maxima than the samples containing K, and also that the former should be better crystallized, as concluded from the larger sharpness of their diffraction peaks. This is due to the co-existence, in the case of the K-samples, of some Mn oxides, probably due to the use of different permanganate/glucose ratios. The inter-crossing of the glucose molecules is lower if low glucose concentrations are used, thus leading to lower interconnection of the incipiently formed manganese oxides; consequently, flocculation of the gel with a larger external surface area is observed, and larger amounts of K ions are extracted from the surrounding medium, and thus non-stoichiometric Mn oxides (with a lower K content) are formed. In addition, low concentrated glucose solutions have a limited reducing ability, and formation of cryptomelane [9], with a higher oxidation state of Mn than in birnessite (3.88 versus 3.63) is favoured. On the other hand, large concentrations of permanganate and glucose favour formation of single gels which act as birnessite precursors after drying and calcination; however, easily flocculating gels are formed with diluted solutions of the reagents, leading to formation of mixtures of cryptomelane and Mn_2O_3, and if the glucose concentration is extremely low, formation of Mn_2O_3 is exclusively observed [9].

In any case, both series of samples (containing potassium or sodium) are more crystalline than those obtained by Mn^{2+} oxidation with hydrogen peroxide, which PXRD diagrams display weak, broad diffraction maxima, due to co-formation of birnessite and MnO(OH) for low cation/manganese ratios [33].

3.3. Thermal analysis

The thermal behaviour of these solids strongly depends on the precise nature of the interlayer cation. In order to assess the processes taking place during thermal decomposition, related to possible oxidation reactions involving manganese cations, the thermal analyses have been carried out both under an oxidative (oxygen) or inert (nitrogen) dynamic atmosphere (Fig. 3). In addition, the PXRD diagrams of solids formed at intermediate temperatures (where the TG curves show a *plateau* indicating formation of stable phases) have been also recorded, in order to identify the crystalline species formed.

TG curves show that, at low temperatures (up to 400 °C) the behaviour of the samples is rather similar, although in the Na-containing samples the weight loss is larger than in those samples containing potassium (Fig. 3); this is due to their larger content in interlayer water, which is removed in this temperature range. The values, however, are lower than in birnessites prepared following other methods [3–7,33], probably because samples prepared by this sol–gel method had been calcined at 400 °C to remove excess of glucose and to form the birnessite structure. For sample VK, such a first weight loss due to interlayer water removal extends up to 600 °C.

This water loss effect is recorded in the DTA curves as a strong endothermic effect centred around 160 °C, and takes place in two steps: the first one, up to ca. 160 °C, corresponds to removal of weakly bonded water molecules (adsorbed on the external surface of the crystallites and uncoordinated interlayer water), and the second one is due to removal of crystallization water. The process is completed at

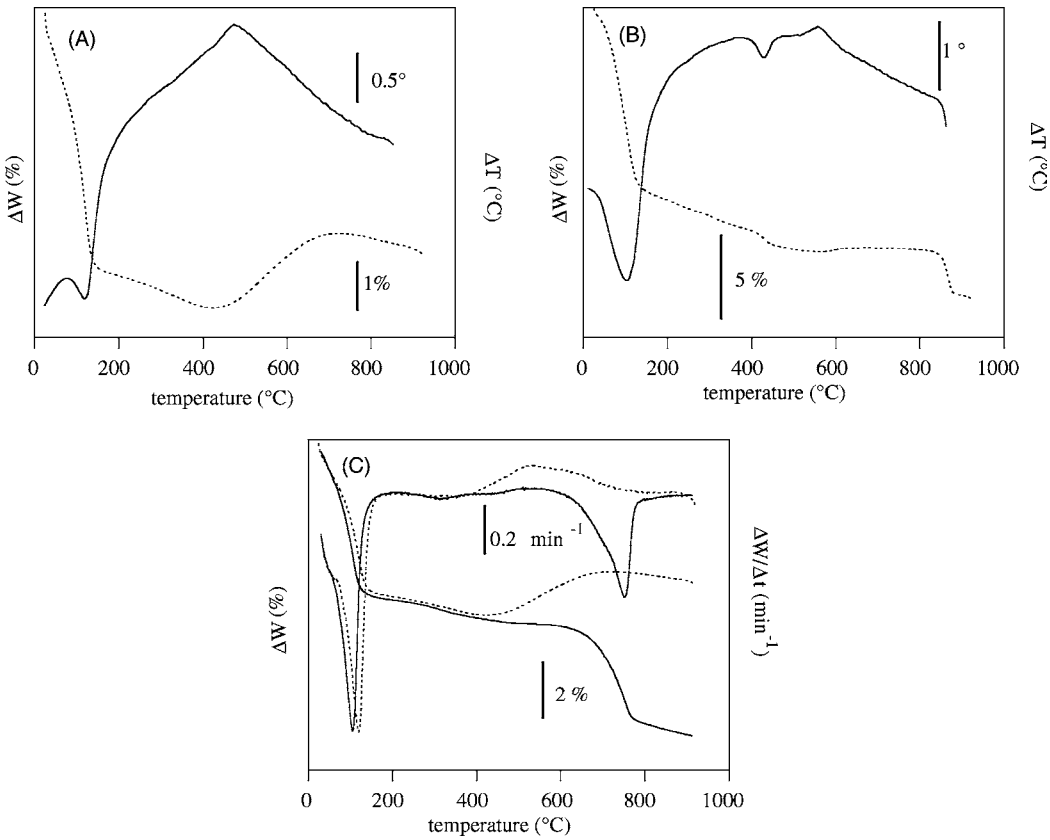

Fig. 3. DTA (solid lines) and TG (dotted lines) curves for samples (A) GK1 and (B) GNa1 in O_2; (C) DTG (top) and TG (bottom) curves for sample GK1 recorded in O_2 (dotted line) and N_2 (solid line).

ca. 400 °C for the K-containing samples (except for sample VK, not shown in Fig. 3), and extends up to 500 °C for the Na-containing ones. Total weight loss in this temperature range has been used to calculate the amount of water given in the structural formulae of the solids (Table 1). In some cases, the DTA peak splits into two minima at 80 and 170 °C [6,35], but in our case it is extremely sharp and does not split. However, the second effect, also due to water release between 160 and 400 °C, gives rise, in the case of the Na-containing samples, to weak DTA minima close to 250 and 340 °C, suggesting that removal of interlayer water molecules is not a simple process.

The DTA curve for the Na-containing sample shows a weak endothermic effect around 470 °C, followed by an even weaker exothermic effect centred around 600 °C. These processes take place with simultaneous weight losses, as the TG curve shows, and, according to Le Goff et al. [34], they are due to formation of metastable phases which, at higher temperatures, lead to formation of solids with a tunnel structure. On the other hand, Feng et al. [5] have claimed that the endothermic effect close to 400 °C is due to partial transformation of the layered oxide to Mn_2O_3, together with evolution of oxygen gas, while the exothermic effect at 600 °C is due to transformation from the layered structure to $Na_{0.44}MnO_2$. Contrary to this behaviour, sample GK1 shows in this temperature range a slight weight increase when the analysis is recorded in oxygen, however, such a weight increase is not recorded when the analysis is performed in nitrogen; instead, a steady weight decrease is recorded up to 600 °C, followed by a sharp weight decrease between 600 and 800 °C. The crystalline phases formed upon

heating in nitrogen and in oxygen at 600 and 800 °C have been determined by PXRD, Fig. 4: in nitrogen, cryptomelane (KMn_8O_{16}, a 2 × 2 tunnel structure) is mostly formed at 600 °C, with minor amounts of Mn_3O_4, which is the major component at 800 °C; on the contrary, in oxygen the phase existing in both cases (calcination at 600 and 800 °C) corresponds to cryptomelane.

3.4. FT-IR spectroscopy

The FT-IR spectra of the samples synthesised are shown in Fig. 5. A broad band is recorded between 3500 and 3200 cm^{-1}, due to the antisymmetric and symmetric stretching modes of hydroxyl groups, both those existing in defects or vertex of the structure, and interlayer water molecules; the band is broad because of hydrogen bondings with different strengths among these species and with the layer oxide anions. Moreover, some of these water molecules could be co-ordinated to the interlayer cations. The band corresponding to the OH stretching mode of water molecules splits in some cases: the main absorption is recorded at 3430 cm^{-1} for sample GK1, with an easily observed shoulder at 3280 cm^{-1}. Such a splitting is even clearer for sample GNa1, with absorptions at 3426 and 3295 cm^{-1}. On the contrary, the shoulder is not clearly recorded for sample GNa1.5, where the strong absorption is recorded at 3445 cm^{-1}. Finally, a sharp absorption is recorded at 3302 cm^{-1} for sample VK. According to Aronson et al. [35], the rather clear splitting of the bands arises from ordering of these water molecules, well because of their interaction with interlayer cations, or well because of restricted movements in the interlayer region.

The weak absorptions below 3000 cm^{-1} are due to C–H stretching modes of organic contamination during handling of the sample to prepare the tablets for recording the spectra. The weak-medium intensity band recorded at 1630 cm^{-1} is due to the deformation mode of water molecules. Intense absorptions are recorded between 600 and 400 cm^{-1}, which are due to Mn–O stretching modes [18,35]. The main absorption is recorded close to 525 cm^{-1}, with a sharp shoulder at 470 cm^{-1} and a weaker one at 425 cm^{-1}, which correspond to Mn–O stretching modes of the octahedra layers in the birnessite structure [35,36].

3.5. Surface texture and specific surface area

Nitrogen adsorption isotherms at −196 °C correspond in all cases to type II in the IUPAC classification [37], characteristic of a non-porous or macroporous absorbent, without restricted monolayer–multilayer adsorption, Fig. 6. These findings indicate that, under the experimental conditions during recording of the isotherms, nitrogen molecules are unable to access to the interlayer region, probably because it is populated with the cations and the water molecules. It should be recalled that also in layered double hydroxides, with a basal spacing close to 7.6 Å, the nitrogen molecules do not enter into the interlayer region [38], and only for systems with larger interlayer spacings and highly charged interlayer anions, interlayer adsorption of nitrogen is observed, leading to type I isotherms, i.e. corresponding to microporous solids. The absence of microporosity is confirmed by the *t*-plots [39], which give rise to straight lines passing through the origin in all cases.

All isotherms here recorded show an hysteresis loop closing at ca. $P/P^o \approx 0.4$, corresponding to type H3 in the IUPAC classification, which is usually associated to adsorption on aggregates of particles with a layered morphology, forming slit-like pores [37], probably related in our case to the lamellar structure of the microcrystallites. It should be recalled that the isotherm recorded for sample VK is similar to those recorded for the other samples, despite the different nature of the reducing agent used during synthesis, and the different properties of this sample, as concluded from the studies carried out by applying other physicochemical techniques.

The BET specific surface areas for these samples are summarized in Table 1. The values for the Na-containing samples is ca. twice those for the K samples. As the samples are not microporous (as concluded from the shapes of the isotherms) because the nitrogen molecules do not access into the interlayer region, this difference can not be attributed to different accessibility to the interlayer region, depending on the size of the interlayer cation (K^+ is obviously larger than Na^+), but probably to the different properties of the gel obtained during the synthesis procedure, as the sodium sample is more consistent and thicker than the potassium one. On the other hand, the potassium samples contain small impurities of

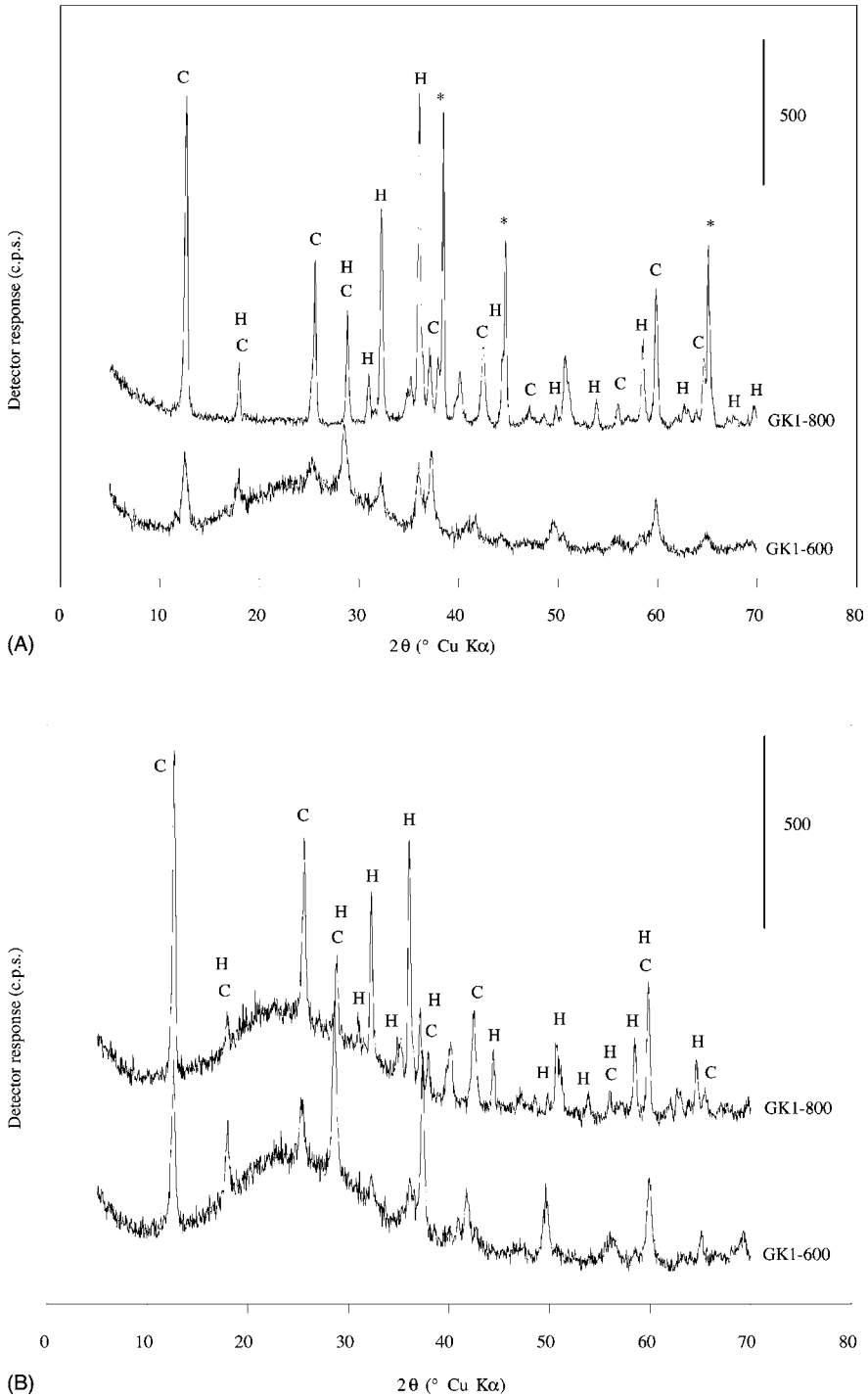

Fig. 4. XRD patterns of sample GK1 calcined in (A) O_2 and (B) N_2 atmosphere (H: Hausmannite, Mn_3O_4; C: Cryptomelane, KMn_8O_{16}) ((*) peaks of Al sampleholder). The patterns have been displaced vertically for clarity.

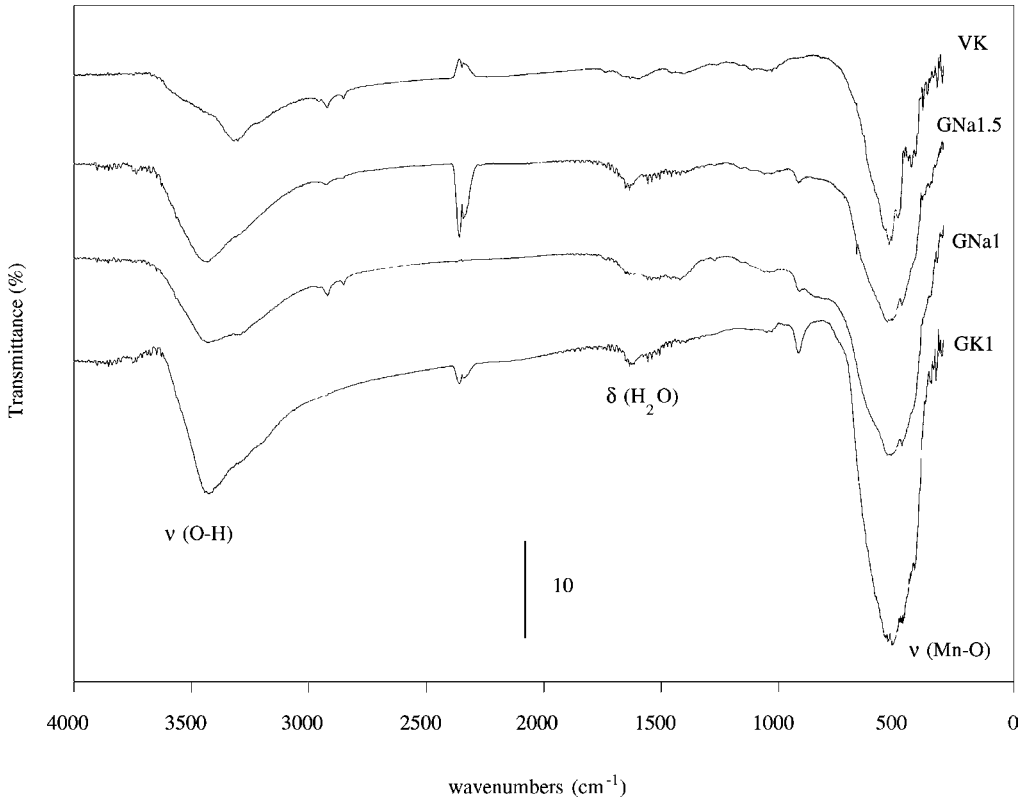

Fig. 5. FT-IR spectra of original birnessite samples. The spectra have been displaced vertically for clarity.

Mn_2O_3, which might be contaminating the samples, probably blocking interparticle pores.

It should be also noted that the specific surface area values are similar for a given interlayer cation, even if different reducing agents have been used (i.e. samples GK1 and VK). The slightly larger S_{BET} value for sample GNa1.5 with respect to sample GNa1 (10%) is probably originated by the larger glucose content during synthesis; during calcination, formation of CO_2 and water vapour takes place, which evolution might have formed pores and chimneys which would account for such a larger specific surface area, in a similar way to surface area developing during calcination of carbonate or nitrate-containing hydrotalcites [40].

Samples prepared using glucose as reducing agent show a bimodal pore size distribution curve, predominating those pores with diameters of 22 and 35 Å; on the contrary, sample VK shows an almost monomodal distribution curve.

3.6. Ion exchange

Results from ion exchange with some of the samples prepared are summarized in Tables 2 and 3. Values are given as percentage exchange. As it can be observed, total exchange is not achieved in any case, and sodium is better exchanged than potassium, although for Li^+ in the case of the sodium-containing samples exchange

Table 2
Results from ion exchange at room temperature, during 24 h and cation concentration 1 M, Molar percentage exchange

Cation	Sample		
	GK1	GNa1	GNa1.5
Mg^{2+}	31	52	58
Cu^{2+}	80	96	98
Li^+	94	98	97

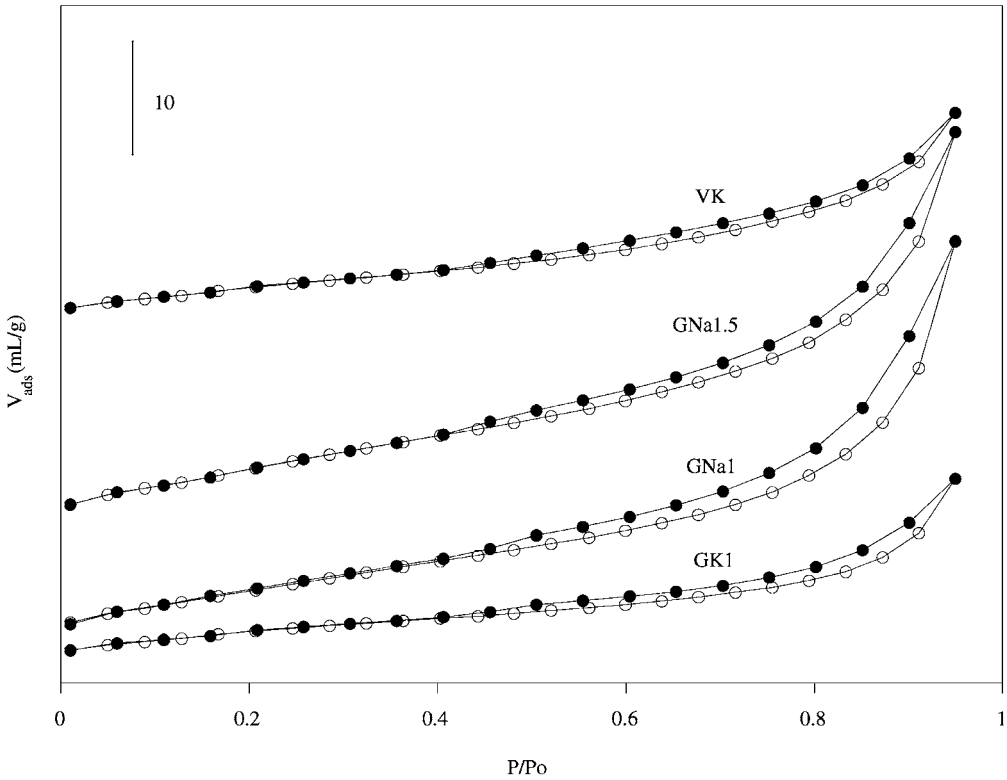

Fig. 6. N_2 adsorption–desorption isotherms at −196 °C for the original samples (empty circles: adsorption; filled circles: desorption). The curves have been displaced vertically for clarity.

was almost complete, and lower exchange levels are reached for Cu^{2+} and even lower for Mg^{2+}. From these results, there is no clear relationship between the size of the exiting cation (Na^+ or K^+) and the entering cation (Li^+, Mg^{2+}, Cu^{2+}), although the lower size of Li^+ may be important to achieve a larger exchange for this cation. However, ionic size of Mg^{2+} and Cu^{2+} are very similar in an octahedral co-ordination and, however, their exchange abilities are different (Mg^{2+} exchanges better than Cu^{2+}), probably because of the larger hydration ability of Mg^{2+} than Cu^{2+}.

Table 3
Results from ion exchange at 80 °C for sample GK1

Cation	Treatment			
	(1 M/3 h)	(1 M/8 h)	(1.5 M/3 h)	(1.5 M/8 h)
Mg^{2+}	58	63	59	60
Cu^{2+}	90	91	90	90
Li^+	75	76	79	75

Molar percentage exchange for different concentrations of entering cation and exchange time.

Golden et al. [13] have related the ease of ion exchange with the hydration state of the starting solid. So, if hydrated samples are used, with a double interlayer water layer and a basal spacing close to 10 Å, exchange is easy, but if the samples are previously degassed at 105 °C the exchange becomes rather difficult due to dehydration and formation of 7 Å solids. However, in our case exchange levels are rather high, despite the samples have a basal spacing close to 7 Å.

Ching et al. [9] have shown that both Na^+ and K^+ are only partially exchanged, although the exchange degree depends on the previous history of the sample; so complete Na^+ exchange could be achieved in samples prepared by the sol–gel method. However, we have found that extraction of Na^+ ions also depends on the nature of the entering ion (see Table 2).

It should be pointed out that the exchange capacity is different for the Na- and K-containing samples. The values calculated from the formula given in Table 1 are 349 and 201 meq/100 g (of dehydrated sample) for the Na- and K-samples, respectively, markedly larger than those reported elsewhere for layered silicates (e.g. saponite, 100 meq/100 g [41]), and of the same order of those previously reported by other authors (240 meq/100 g for a Na-birnessite [13]). The rather large layer charge density, stabilising the 7 Å distance against expansion to 10 Å, could be responsible for the lack of busserite formation during ion exchange.

The results obtained when the ion exchange is carried out at 80 °C are shown in Table 3. These studies have been carried out only on sample GK1. Whichever the concentration of the solution or the contact time, larger exchange percentages are observed for Mg^{2+} and Cu^{2+}. Opposite results are observed for incorporation of Li^{+}: the exchange percentage was lower than when exchange was carried out at room temperature in all cases. These small changes are in agreement with previous reports by Ching et al. [9], who have shown that an increase in the contact time or the exchange temperature does not strongly modify the exchange process.

PXRD studies of the exchanged samples have shown that the layered structure is maintained, and in all cases diffraction maxima close to 7 and 3.5 Å, due to diffraction by planes (0 0 1) and (0 0 2), respectively, of birnessite materials are recorded, suggesting a topotactic reaction. However, a detailed study of the diagrams shows minor changes in the precise position of these maxima, depending on the entering cation, and so, a slightly lower spacing is observed for the Mg-containing exchanged material. When the original samples had been obtained by processes different from the sol–gel, busserites with basal spacings close to 10 Å could be obtained from Na-containing birnessites, probably because the additional layer of water molecules in some sort of way favours mobility of the entering cations. This process should be especially important in the case of highly hydrated cations, such as Mg^{2+} [20,42–45]. PXRD diagrams for samples exchanged at a higher temperature and changing the contact time or the concentration of the salt do not differ significantly from those for the samples prepared by ion exchange at room temperature.

No microporosity develops in any case in the exchanged samples; all them correspond to type II in the IUPAC classification [37], as for the original, non-exchanged samples. However, the specific surface areas are different, depending on the entering cation (Table 1). Incorporation of magnesium leads in all cases to a small increase in S_{BET}. The behaviour observed for the Cu-samples is somewhat erratic, largely increasing for GK1, does not change for GNa1.5, but the S_{BET} is the same as for the Mg-exchanged sample, when starting from GNa1. However, the specific surface areas for the Li-containing samples are, in all cases, very much larger than for the other samples, exchanged or not; values are even twice those for the non-exchanged samples (GK1 and GNa1). This result is rather surprising, as no important crystallinity change can be concluded from the PXRD diagrams for these samples. However, the pore size distribution curves [46], show an important development of pores with a diameter close to 40 Å for the Li-containing samples, which is not observed in other cases. So, we may tentatively conclude that exchange takes place topotactically, without destroying the lamellar structure of the starting solid, but it acts as a further ageing process, modifying the external surface area (N_2 molecules do not access inside the interlayer space), although further experiments are required to reach a definitive conclusion.

3.7. Calcined systems

One of the most important properties of these birnessites is their ability to transform to tunnel-like and spinel structures upon heating under controlled conditions [13,26,47]. The Li–Mn spinels obtained so far have demonstrated their role in rechargeable lithium batteries [22–25]. We have characterised the solids obtained upon calcination of some of our samples at 600 and 1000 °C, as the thermal study described above has shown the existence of thermal effects, due to transformations, between these two temperatures.

The PXRD patterns of the uncalcined solids, and of those calcined at 600 and 1000 °C for pristine materials GK1 and GNa1.5 are shown in Fig. 7. Calcination even at 600 °C destroys the layered structure, forming highly crystalline solids. It has been previously shown that the precise nature of the solids formed upon calcination depends on the nature of the interlayer cation;

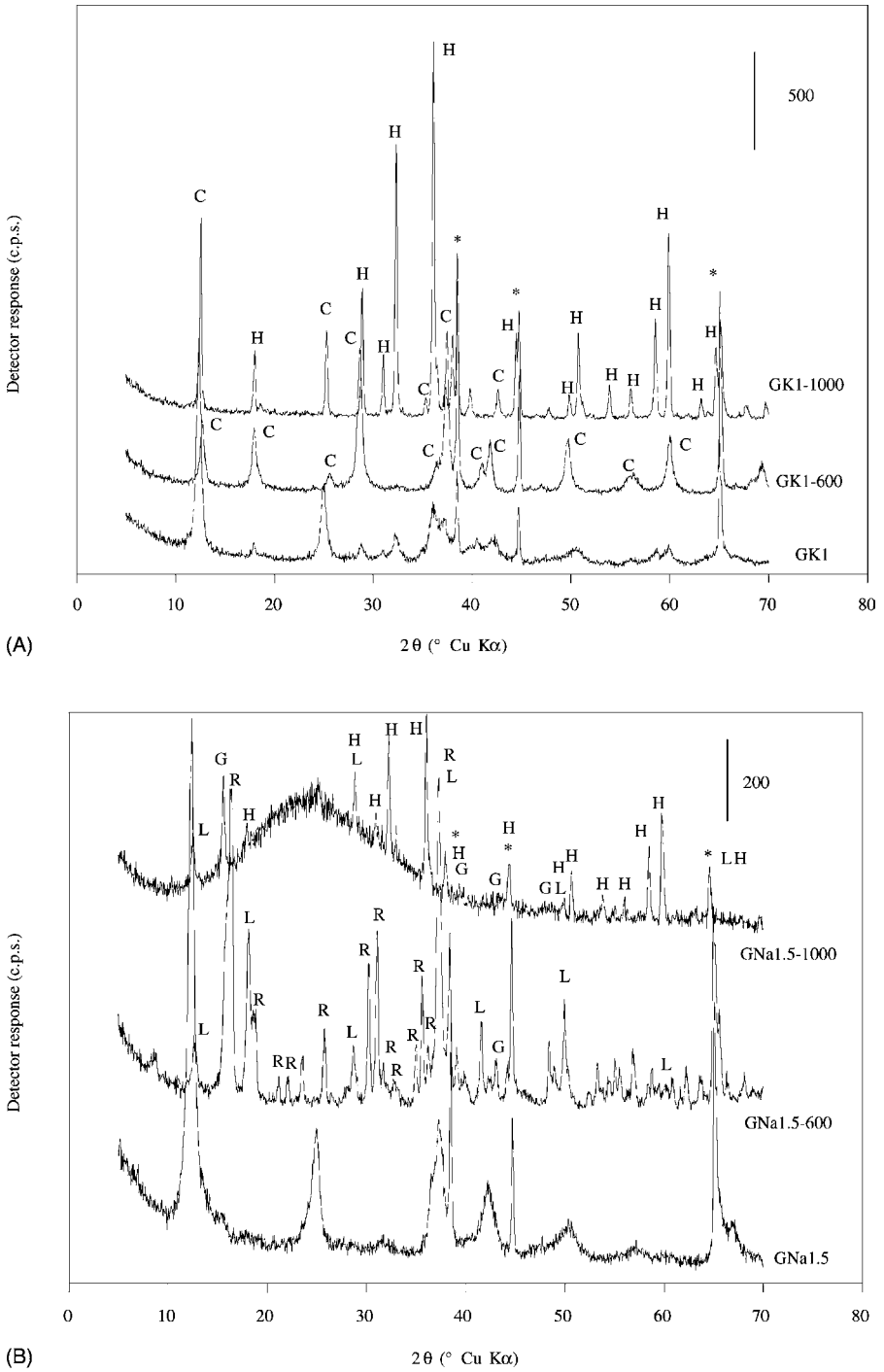

Fig. 7. XRD patterns of samples (A) GK1 and (B) GNa1.5 calcined at 600 and 1000 °C (the patterns for the original solids are also shown; (*): peaks of Al sampleholder; C: Cryptomelane, H: Huasmannite, L: Hollandite, R: Romanechite, G: layered hexagonal $Na_{0.7}MnO_{2.05}$), The patterns have been displaced vertically for clarity.

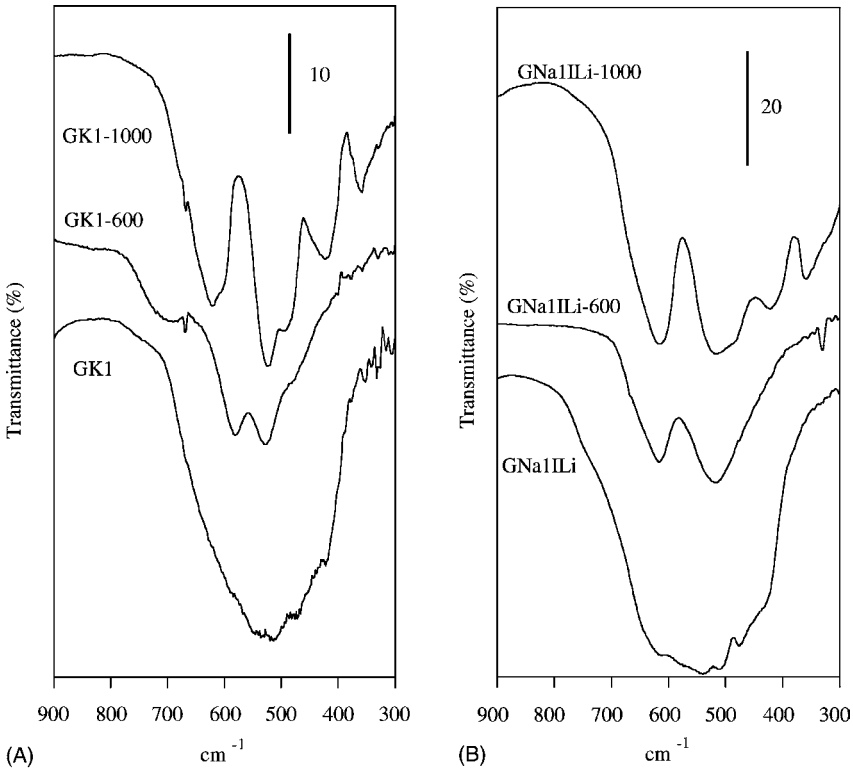

Fig. 8. FT-IR spectra of samples (A) GK1 and (B) GNa1.5 calcined at 600 and 1000 °C. The spectra have been displaced vertically for clarity.

Golden et al. [13] have shown that tunnel structures (hollandite) are formed when bulk cations (e.g. K^+, Ba^{2+}) exist in the interlayer, while if the interlayer cation is smaller (Li^+, Mg^{2+}) then bixbyte or hausmannite structures are formed. However, calcination of Li-containing birnessites may lead to formation of cryptomelane, which thermal stability is lower than that of the material obtained from K-birnessites. Ching et al. [9] have reported that upon heating, the lamellar structure collapses around the interlayer cation, and the structure of the final solid depends on the ionic radius of this cation, potassium possessing the right size for cryptomelane formation. Golden et al. [13] have reported that destruction of the layers starts at a lower temperature (even 200–400 °C, although in our case this should not apply, as the samples had been originally calcined at 400 °C), but cryptomelane is only formed above 600 °C. The PXRD diagram of sample GK1-600 shows only diffraction maxima due to cryptomelane, and this is the single phase identified by FT-IR spectroscopy (Fig. 8), with characteristic Mn–O stretching bands at 690, 675, 583, and 529 cm^{-1} [36]. As for sample GK1ILi the exchange was very high, the PXRD diagram of the sample calcined at 600 °C shows the formation almost exclusively of the $LiMn_2O_4$ spinel, with only extremely low amounts of bixbyte and cryptomelane.

The behaviour observed for sample GK1IMg is rather similar to that for the unchanged sample, cryptomelane and small amounts of $MgO–Mn_2O_3$ (JCPDS: 23-392) [30] forming at 600 °C; formation of cryptomelane should be favoured by the poor K/Mg exchange in this sample. The oxide identified by PXRD, $MgO–Mn_2O_3$, is a mixed Mn–Mg oxide with a tetragonal structure. Finally, a cryptomelane–bixbyte mixture is formed upon calcination of sample GK1ICu at 600 °C, together with a small amount of a $Cu_{1.5}Mn_{1.5}O_4$ spinel.

The layered structure is also destroyed for the Na-samples calcined at 600 °C. However, some of the maxima recorded are slightly broad, indicating that the corresponding solids are not as crystalline as those obtained at 600 °C from the K-containing precursors. Many weak, sharp peaks have not been undoubtedly assigned to a determined compound, because of the many and different non-stoichiometric Na–Mn–O compounds able to be formed [48,49]. The glucose/cation ratio does not modify the qualitative nature of the phases existing in the calcined solids, and only minor changes in the intensity and/or broadness of some of the peaks can be observed. Sample GNa1ILi-600 shows diffraction maxima exclusively due to the $LiMn_2O_4$ spinel, and no peak corresponding to other Mn-containing oxides could be detected. The FT-IR data are in agreement with this finding, as two intense well defined bands are recorded at 617 and 516 cm^{-1}, due to modes ν_2 and ν_4 of this Li–Mn spinel [50].

Major formation of Mn_3O_4 is observed when the samples are calcined at 1000 °C, although, depending on the interlayer cation, some weak peaks due to cryptomelane (K samples) or non-stoichiometric Na–Mn oxides (Na samples), are also recorded. Consequently, the FT-IR spectra show development of new bands at 621, 524, 422, and 358 cm^{-1}, due to modes ν_1, ν_2, ν_3 and ν_4 of the Mn_3O_4 spinel. The weak bands recorded should be undoubtedly due to the minor impurities.

4. Conclusions

Crystalline birnessites containing Na^+ or K^+ in the interlayer have been obtained by the sol–gel method, starting from glucose, polyvinylalcohol and permanganate salts. The Na- samples are more crystalline, probably because the synthesis is in this case less sensitive to the experimental synthesis conditions, especially the permanganate/glucose ratio. Ion exchange is easier for the Na samples than for the K ones, and almost complete Na/Li is achieved, while exchange for Mg or Cu is weaker, probably because of the radius of the entering cation and the hydration degree of the interlayer.

These samples are thermally stable up to 400–500 °C; spinels and tunnel structure are formed above this temperature. Cryptomelane, together with small amounts of bixbyte and Li or Cu spinels, are formed for samples containing K in the interlayer (together with Li or Cu by ion exchange); mixed Mg–Mn oxides are formed in the case of samples containing Mg in the interlayer. Whichever the initial glucose/cation ratio, no appreciable differences are observed in the calcined Na samples. However, we should point out formation of $LiMn_2O_4$ upon calcination of the Na/Li sample at 600 °C. No microporosity was found in any case.

Acknowledgements

Financial support from DGES (PB96-1307-C03-01) is acknowledged.

References

[1] Q. Feng, H. Kanoh, Y. Mijay, K. Ooi, Chem. Mater. 7 (1995) 1226.
[2] Q. Feng, H. Kanoh, Y. Mijay, K. Ooi, Chem. Mater. 7 (1995) 1722.
[3] Q. Feng, K. Yanagisawa, N. Yamasaki, J. Chem. Soc., Chem. Commun. (1996) 1607.
[4] Q. Feng, K. Yanagisawa, N. Yamasaki, J. Ceram. Soc. Jpn. 104 (1996) 897.
[5] Q. Feng, E.H. Sun, K. Yanagisawa, N. Yamasaki, J. Ceram. Soc. Jpn. 105 (1997) 564.
[6] Q. Feng, K. Yanagisawa, N. Yamasaki, J. Mater. Sci. Lett. 16 (1997) 110.
[7] Q. Feng, K. Yanagisawa, N. Yamasaki, J. Porous Mater. 5 (1998) 153.
[8] Q. Feng, H. Kanoh, K. Ooi, J. Mater. Chem. 9 (1999) 319.
[9] S. Ching, D.J. Petrovay, M.L. Jorgensen, S.L. Suib, Inorg. Chem. 36 (1997) 883.
[10] S. Ching, J.A. Landrigan, M.L. Jorgensen, N. Duan, S.L. Suib, Chem. Mater. 7 (1995) 1604.
[11] S. Ching, S. Roark, J.L. Duan, S.L. Suib, Chem. Mater. 9 (1997) 750.
[12] R.M. Mckenzie, Mineral. Mag. 38 (1971) 493.
[13] D.C. Golden, J.B. Dixon, C.C. Chen, Clays Clay Miner. 34 (1986) 511.
[14] J.E. Post, D.R. Veblen, Am. Mineral. 75 (1990) 477.
[15] R. Giovanoli, E. Stähli, W. Feitknecht, Helv. Chim. Acta 53 (1970) 209.
[16] J. Luo, A. Huang, S.H. Park, S.L. Suib, C.L. O'Young, Chem. Mater. 10 (1998) 1561.
[17] R.M. Cornell, R. Giovanoli, Clays Clay Miner. 36 (1988) 249.
[18] K. Kuma, A. Usui, W. Paplawsky, B. Gedulin, G. Arrhenius, Mineral. Mag. 58 (1994) 425.
[19] P.L. Goff, N. Baffier, S. Bach, J.P.P. Ramos, J. Mater. Chem. 4 (1994) 875.

[20] P.L. Goff, N. Baffier, S. Bach, J.P.P. Ramos, Mater. Res. Bull. 31 (1996) 63.
[21] S. Thu, G.J. Racz, T.B. Goh, Clays Clay Miner. 42 (1994) 321.
[22] Y.K. Sun, S.H. Jin, J. Mater. Chem. 8 (1998) 2399.
[23] J.R. Dahn, U.V. Sacken, M.W. Juzkow, H. Al-Janaby, J. Electrochem. Soc. 138 (1991) 2207.
[24] A.R. Armstrong, H. Huang, R.A. Jennigs, P.G. Bruce, J. Mater. Chem. 8 (1998) 255.
[25] M.H. Rossouw, D.C. Liles, M.M. Thackeray, W.I.F. David, S. Hull, Mater. Res. Bull. 27 (1992) 221.
[26] R.N. DeGuzman, Y.F. Shen, E.J. Neth, S.L. Suib, C.L. O'Young, S. Levine, J.M. Newsam, Chem. Mater. 6 (1994) 815.
[27] C.N.R. Rao, A.K. Cheetham, R. Mahesh, Chem. Mater. 8 (1997) 2421.
[28] Y.F. Shen, R.P. Zerger, R.N.D. Guzman, S.L. Suib, L. McCurdy, D.I. Potter, C.L. O'Young, Science 260 (1993) 511.
[29] Y.G. Yin, W.Q. Xu, Y.F. Shen, S.L. Suib, Chem. Mater. 6 (1994) 1808.
[30] JCPDS. Joint Committee on Powder Diffraction Standards, International Centre for Diffraction Data, 1977, Pennsylvania, USA.
[31] S. Lowell, J.E. Shields, Powder Surface Area and Porosity, Chapman and Hall, London, 1984.
[32] V. Rives, Adsorption Sci. Technol. 8 (1991) 95.
[33] O. Prieto, Preparación, caracterización y evolución estrustural con la calcinación de óxidos mixtos de manganeso, Ph.D. Thesis, Universidad de Salamanca, Spain, 2001.
[34] P.L. Goff, N. Baffier, S. Bach, J.P.P. Ramos, R. Messina, Solid State Ion. 61 (1993) 309.
[35] B.J. Aronson, A.K. Kinser, S. Passerini, W.H. Smyrl, A. Stein, Chem. Mater. 11 (1999) 949.
[36] R.M. Potter, G.R. Rossman, Am. Mineral. 64 (1979) 1199.
[37] K.S.W. Sing, D.H. Everett, R.A.W. Haul, L. Moscou, R.A. Pierotti, J. Rouquerol, T. Siemieniewska, Pure Appl. Chem. 57 (1985) 603.
[38] V. Rives, in: Layered Double Hydroxides: Present and Future, Nova Science Publishers Inc., New York, 2001, p. 229.
[39] B.C. Lippens, J.H. d. Boer, J. Catal. 4 (1965) 319.
[40] E.C. Kruissink, L.J.V. Reijden, J.R.H. Ross, J. Chem. Soc., Faraday Trans. 1 77 (1981) 649.
[41] O. Prieto, M.A. Vicente, M.A. Bañares-Muñoz, J. Porous Mater. 6 (1999) 335.
[42] Y.F. Shen, S.L. Suib, C.L. O'Young, J. Am. Chem. Soc. 116 (1994) 11020.
[43] D.C. Golden, C.C. Chen, J.B. Dixon, Science 231 (1986) 717.
[44] D.C. Golden, C.C. Chen, J.B. Dixon, Clays Clay Miner. 35 (1987) 271.
[45] A.D. Wadsley, J. Am. Chem. Soc. 72 (1950) 1781.
[46] R.W. Cranston, F.A. Inkley, Adv. Catal. 9 (1957) 143.
[47] C.C. Chen, D.C. Golden, J.B. Dixon, Clays Clay Miner. 34 (1986) 565.
[48] J.P. Parant, R. Olazcuaga, M. Devalette, C. Fouassier, P. Hagenmuller, J. Solid State Chem. 3 (1971) 1.
[49] L. Liu, Q. Feng, K. Yanagisawa, Y. Wang, J. Mater. Sci. Lett. 19 (2000) 2047.
[50] S.R.S. Prabaharan, S.S. Michael, C. Julien, J. Inorg. Mater. 1 (1999) 21.